Available online at www.sciencedirect.com

SCIENCE DIRECT®

Surface & Coatings Technology 186 (2004) 112–117

SURFACE & COATINGS TECHNOLOGY

www.elsevier.com/locate/surfcoat

Molybdenum–carbon film fabricated using metal cathodic arc and acetylene dual plasma deposition

Ricky K.Y. Fu[a], Y.F. Mei[a], L.R. Shen[a,b], G.G. Siu[a], Paul K. Chu[a,*], W.Y. Cheung[c], S.P. Wong[c]

[a] *Department of Physics and Materials Science, City University of Hong Kong, Tat Chee Avenue, Kowloon, Hong Kong*
[b] *Southwestern Institute of Physics, Chengdu, Sichuan 610041, China*
[c] *Department of Electronic Engineering, Chinese University of Hong Kong, Shatin, Hong Kong*

Available online 24 May 2004

Abstract

Metal cathodic arc and acetylene dual plasma deposition is used to synthesize molybdenum-containing diamond-like carbon (Mo-DLC) thin films. The Mo contents in the film layer can be controlled by varying the acetylene gas flow rates and the substrate bias voltages. The Mo-doped film prepared by the above technique exhibits small surface roughness. Fine molybdenum carbide grains are found to be embedded inside the amorphous carbon cross-linked structures. In addition, these films are shown to possess high thermal stability after a series of high temperature annealing. The results show that dual plasma deposition is a useful and effective technique to fabricate metal-incorporated carbon thin films with controlled metal contents.

Keywords: Dual plasma deposition; Diamond-like carbon films (DLC); Metal-doped DLC; Nanocrystalline carbides; Thermal stability

1. Introduction

Metal-doped diamond-like carbon (Me-DLC) films have attracted a great deal of scientific interest for more than a decade [1,2]. As the metallic nanocrystalline clusters [3] and metallic carbide nanocrystallites [4] are present in the amorphous carbon matrix, metal-containing DLC films exhibit several superior properties such as good adhesion with the substrate [5], high hardness [6], low friction coefficient [7], high thermal stability [8] and high electrical conductivity [9]. The reason for the good film adhesion is that metal doping can lower the compressive stress in the carbon cross-linked structure [10]. In addition, the nano-clusters in the film can further stop and hinder cracks initiation and propagation so as to yield high film toughness [11]. The conductivity of the film varies with the amount of the incorporated metals and can be explained using the Poole-Frenkel effect [12] that is enhanced by metal precipitates in the DLC film thereby providing extra paths for electronic transportation [13]. Several techniques have been proposed to deposit metal-doped DLC films. The most common methods include magnetron assisted pulsed laser deposition [14], sputter deposition using a hydrocarbon gas [15], radiofrequency (RF) magnetron sputtering [16], and electron cyclotron resonance chemical vapor deposition (ECR-CVD) with metal grids [17,18].

Recently, we attempt to deposit metal-doped DLC using hybrid plasma deposition in an immersion configuration. The metal cathodic arc is used primarily to produce the metal plasma and the reactant gases are fed in the vicinity of the metal plasma plume. In our process, the dual plasma is generated by the vacuum arc in contrast with that generated by two plasma sources in other studies [19–21]. The plasmas are guided and transported through a curved duct [22,23] into the process chamber to conduct deposition. In this paper, we report the deposition and characterization of molybdenum-containing diamond-like carbon (Mo-DLC) thin films. The experiments were carried out with different acetylene (C_2H_2) gas flow rates and sample bias voltages. Several analytical techniques including Rutherford back-scattering spectrometry (RBS), contact mode atomic force microscopy (AFM), X-ray photoelectron spectroscopy (XPS), X-ray diffraction (XRD) and laser Raman scattering

* Corresponding author. Tel.: +852-27-887724; fax: +852-27-889549/852-27-887830.
E-mail address: paul.chu@cityu.edu.hk (P.K. Chu).

0257-8972/$ - see front matter © 2004 Elsevier B.V. All rights reserved.
doi:10.1016/j.surfcoat.2004.04.024

were used to verify the process efficacies and characterize the thin films.

2. Experimental

Si (100) was used as the substrate materials. The base pressure in the vacuum chamber was about 1×10^{-5} Torr. Before deposition, the samples were cleaned by an argon plasma for 10 min using a sample bias of -1000 V. Deposition was carried out using a dual plasma consisting of acetylene and metal ions from the cathodic arc source. Acetylene gas was first bled into the vacuum chamber at different flow rates at the vicinity of the exit of the metal arc discharge plume as shown in Fig. 1. In this way, the gas plasma was simultaneously induced when the cathodic arc was triggered. The arc was ignited within the pulse duration of about 300 μs and repetition rate of 60 Hz. The amount of the molybdenum discharge was controlled by the main arc current between the cathode and anode. The plasma was guided into the vacuum chamber by an electromagnetic field. The duct was biased to -20 V to build up a lateral electric field while the external solenoid coils wrapped around the duct produced the axial magnetic field with the magnitude of 100 G. The samples were positioned about 15 cm away from the exit of the plasma stream and they were negatively biased to different voltages.

The Rutherford backscattering spectrometry (RBS) work was carried out using a 2 MeV $^4He^{++}$ beam and a back-scattering angle of 170° to determine the Mo and C contents as well as the film thickness. Contact mode atomic force microscopy (AFM) was conducted on a Park Scientific Instrument (PSI) Autoprobe Research System to evaluate the surface morphology and the scanned area was 0.2×0.2 μm. Mo and C bonding information was acquired using X-ray photoelectron spectroscopy (XPS) employing monochromatic Al K α radiation. Prior to the analyses, the sample surface was cleaned by 4 keV Ar ion bombardment for 1 min to remove atmospheric contaminants. The microstructure of the films was determined by X-ray diffraction (XRD) using a Siemens D500/501 thin film diffractometer with a Cu K α source. In order to evaluate the thermal stability of the deposited films, the samples were cut into small pieces and annealed at a series of different temperatures under nitrogen. Raman scattering spectra were ac-

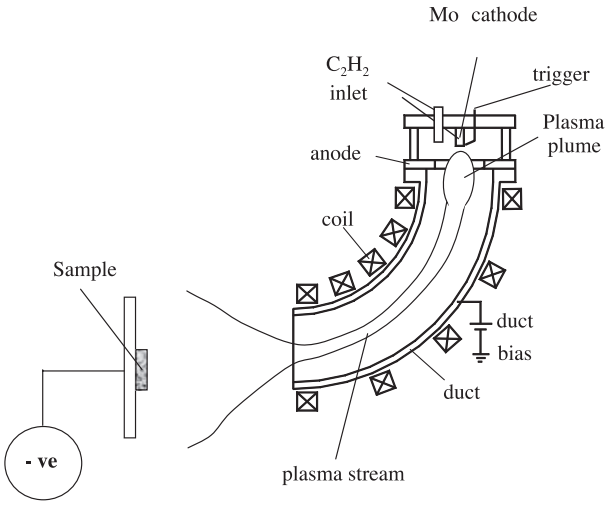

Fig. 1. Schematic diagram of the experimental setup illustrating that C_2H_2 is bled into the vacuum chamber in the vicinity of the Mo plasma plume.

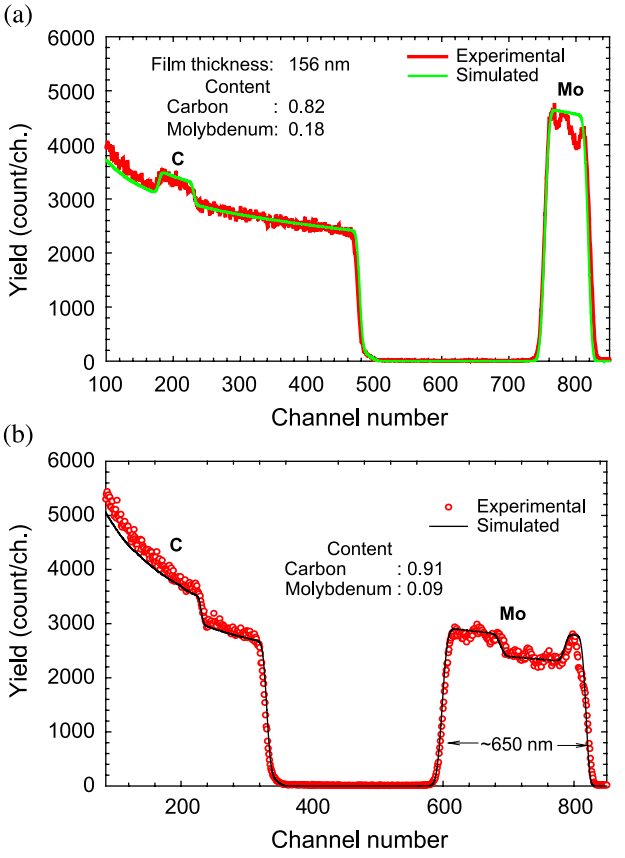

Fig. 2. RBS spectra acquired from the Mo-doped DLC deposited using different C_2H_2 flow rates at substrate bias voltage of -200 V: (a) 5 sccm and (b) 15 sccm.

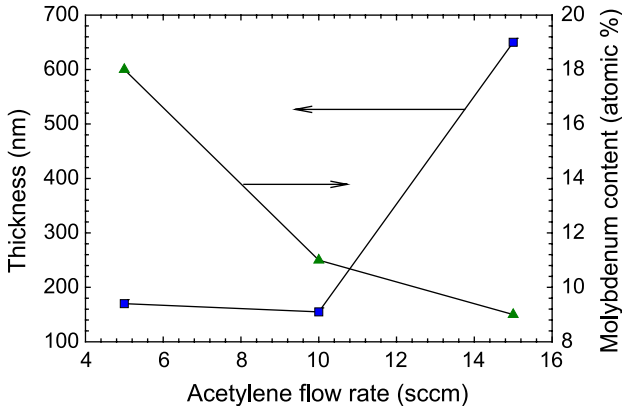

Fig. 3. Film thickness and Mo concentrations in the film as a function of C_2H_2 flow rate at a substrate bias voltage of -200 V.

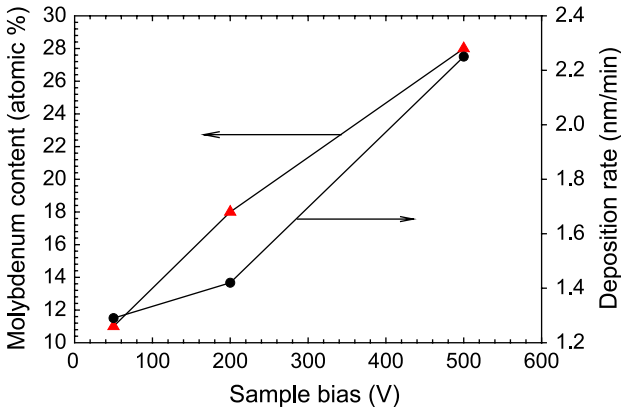

Fig. 4. Mo content in the film as the function of the substrate bias voltage at a C_2H_2 flow rate of 5 sccm.

quired from the films excited by an Ar^+ laser at 514.5 nm using a Jobin Yvon T64000 system.

3. Results and discussion

In order to determine the contents and profiles of Mo and C in the films, RBS analysis was performed and the spectra were fitted using the RUMP simulation code [24]. Fig. 2 depicts the two spectra acquired from the samples deposited at different C_2H_2 flow rates. As the carbon signal overlaps with that of silicon, the error in the carbon concentration is around several atomic % while that of molybdenum is expected to be much lower. It can be observed that molybdenum is quite uniformly distributed in the carbon matrix in our samples prepared under different C_2H_2 flow rates and substrate biases. Generally, in the cathodic arc discharge, molybdenum macro-particles are emitted from the cathode surface. However, these macro-particles are effectively filtered by the curved electromagnetic duct and only the fully ionized molybdenum plasma is guided and transported to the processing chamber. The process efficacy can be evaluated according to the simulation results of the molybdenum contents in the layer. Fig. 3 shows the influence of the C_2H_2 flow rates on the deposited layer thickness and Mo contents. When more C_2H_2 is added to the plasma plume, the layer thickness increases while the Mo concentration decreases. As the C_2H_2 flow rate increases, a higher partial pressure of C_2H_2 ensues in the duct and there are more collisions between the Mo and C_2H_2 as well as species in the C_2H_2 plasma plume. Thus the film thickness increases and Mo fractions

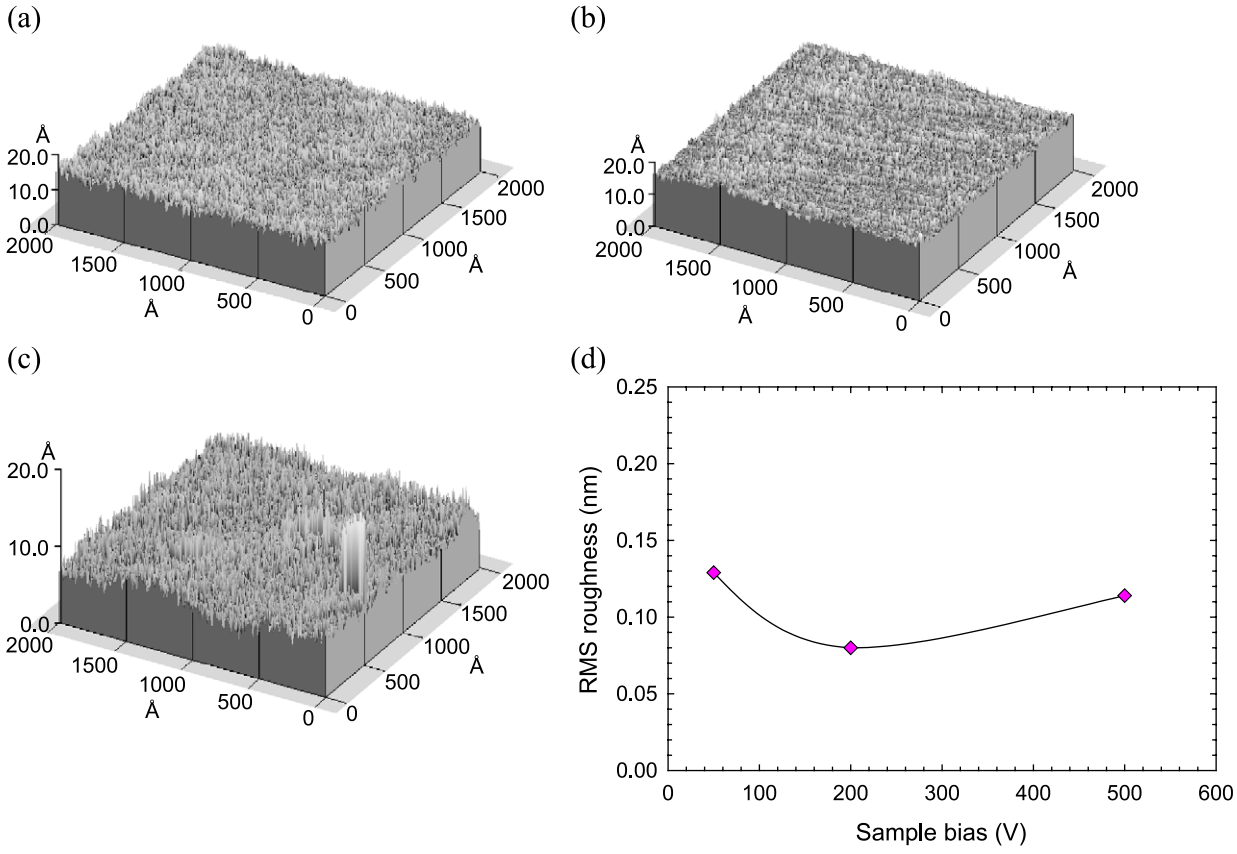

Fig. 5. Surface morphology of Mo-doped DLC deposited at different substrate bias voltages at a C_2H_2 flow rate of 5 sccm: (a) −50 V, (b) −200 V, and (c) −500 V. (d) Shows the RMS surface roughness as the function of the substrate bias voltage.

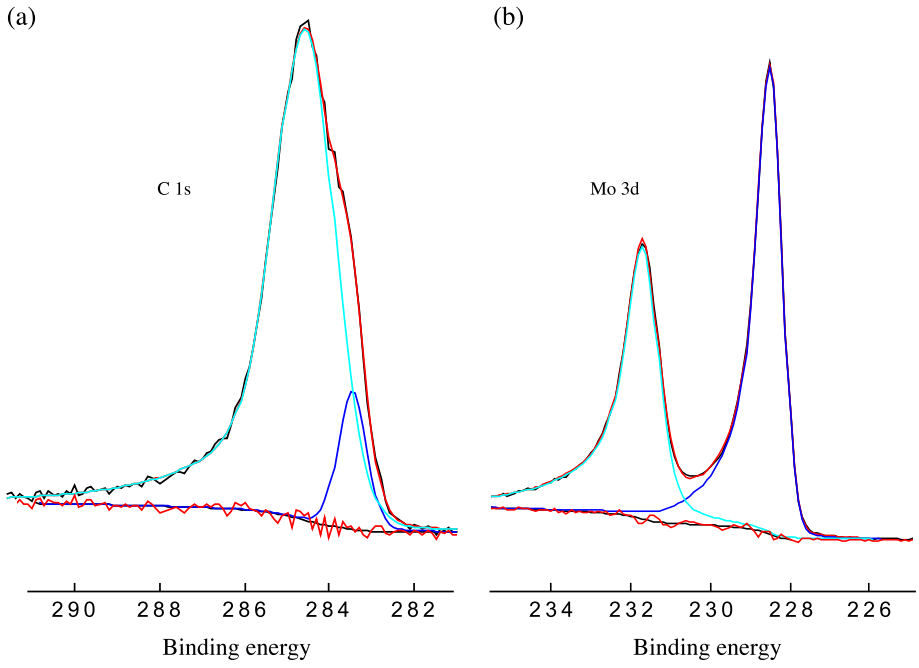

Fig. 6. XPS data showing the C 1s and Mo 3d peaks acquired from the sample deposited at a C_2H_2 flow rate of 5 sccm at a substrate bias voltage of − 200 V.

decreases. Fig. 4 indicates that there is generally an increase of Mo concentration when the bias voltage of sample goes up. Our results are consistent with those of Rusli et al. [17] who deposited metal-containing DLC using an ECR-CVD system. It should, however, be noted that the metal contents in the carbon film are relatively independent of the bias voltage using a magnetron sputter deposition system [25]. It may be attributed to two factors: sputtering effects and electrical adsorption. The ions get higher energies and bombard the deposited films more intensively under a higher sample bias [26]. Thus, the deposited carbon is more severely sputtered, consequently leading to a relatively higher Mo concentration. On the other hand, a higher sample bias results in the incorporation of more ions (including Mo ions and carbon-based ions) relative to the deposited excited carbon-based particles so that the deposition rate increases as illustrated in Fig. 4. From this viewpoint, the Mo contents in the carbon matrix can be controlled by varying the C_2H_2 flow rates and substrate bias voltage.

Fig. 5 demonstrates the surface morphology of Mo-a.C:H films deposited under different substrate biases at 5 sccm C_2H_2 flow rate. It shows that ultra smooth films with a surface root mean square (RMS) roughness of less than 0.15 nm can be obtained using the dual plasma technique. It also reveals that there are no large Mo clusters in the film and the Mo macro-particles (usual size in the range of micrometers) generated from the cathodic arc source have been effectively removed. In fact, there are minor effects of the bias voltage on the surface roughness as shown in Fig. 5d and this may be due to the different deposition rates under various bias voltages.

Fig. 6 displays the XPS results of the C 1s peak and Mo 3d peaks. The C 1s peak can be deconvoluted into two distinct components. Based on previous reports [18,27,28], the first component at a lower binding energy of 283.46 originates from Mo–C whereas the second component with the binding energy of 284.56 corresponds to polymeric carbon. As the Mo–C bond is long and Mo has a weak effect on the C 1s electrons, part of the photo-emitted C 1s

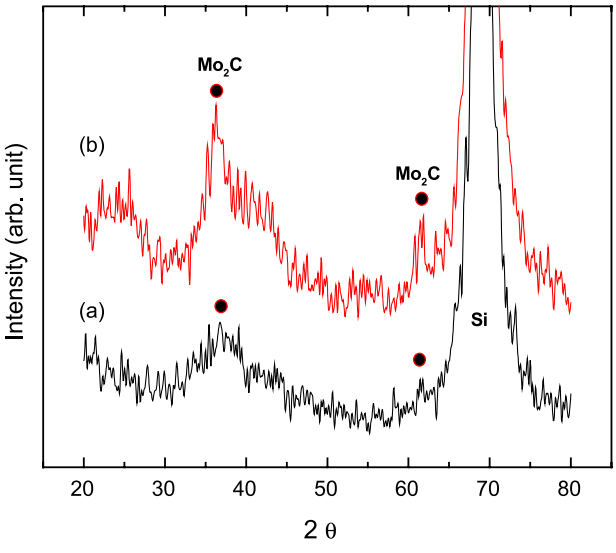

Fig. 7. XRD spectra acquired from Mo-doped DLC deposited at a C_2H_2 flow rate of 5 sccm and substrate bias voltage of − 50 V: (a) as-deposited and (b) annealed at 400 °C for 2 h.

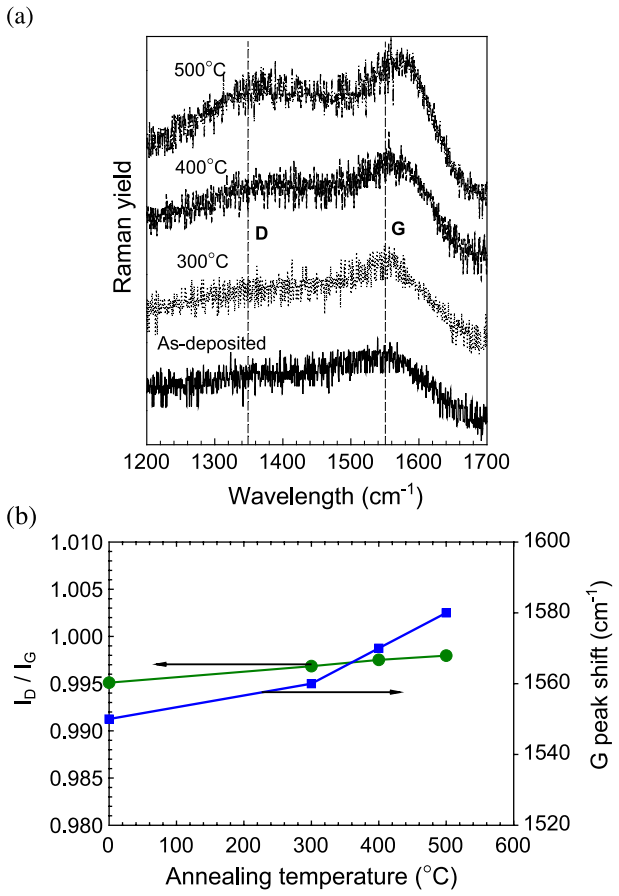

Fig. 8. Surface structure of deposited DLC films: (a) the evolution of Raman scattering results acquired from Mo-doped DLC deposited at a C_2H_2 flow rate of 5 sccm and substrate bias voltage of −50 V after annealing at different temperature (b) I_D/I_G ratio and G peak shift as a function of the annealing temperature.

electrons will have a low binding energy. The Mo 3d peaks in Fig. 6b reveal that the Mo–Mo structures at binding energies of 228.46 and 231.69 are attributed to different electronic spins. As shown in the XRD results in Fig. 7, molybdenum carbide nanocrystallites are formed in the film mainly in the form of Mo_2C phases with multiple orientations. The broad diffraction peak at around 37° may consist of different phases and can be ascribed to a small grain size of the nanocrystalline metallic carbides. The diffraction peaks become relatively sharp and intense after annealing at 400 °C under nitrogen ambient for 1 h. It may mean that more metallic carbides have formed and the grains become large.

We have hitherto demonstrated that molybdenum carbide embedded amorphous DLC films can be fabricated using the dual plasma technique. The samples were subsequently annealed in a furnace at different temperatures under nitrogen and subsequently examined using argon laser Raman scattering. The results are shown in Fig. 8. The films exhibit relatively high thermal stability and only minor variations of carbon clusters and G shift can be observed. As depicted in Fig. 8b, the I_D to I_G ratios and G peak shift suggest that the films become more graphite-like when the annealing temperature increases. The rate of conversion to graphite-like structures in our metal-doped films is, however, low compared to that of the pure DLC annealed at the same temperatures [29,30]. It implies that the metal species incorporated into the carbon matrix retards the transformation of the carbon matrix during the annealing processes.

4. Conclusion

Mo-doped carbon films (Me-C:H) have been synthesized using a dual plasma technique. The experimental results show that the Mo concentration can be controlled by varying the C_2H_2 flow rates and substrate bias voltages. Molybdenum is observed to be relatively uniformly distributed throughout the deposited layer and the films exhibit extremely smooth surface and high thermal stability. XPS and XRD results show that metallic carbide is formed inside the amorphous carbon matrix. Further work to determine the other properties of the films such as mechanical, optical, conductive properties are being conducted in our laboratory.

Acknowledgements

The work was jointly supported by Hong Kong Research Grants Council Competitive Earmarked Research Grant (CERG) #CityU 1137/03E (CityU designation 9040796), Hong Kong Strategic Research Grant (SRG) #7001447, and National Natural Science Foundation of China under Grant No. 10275020.

References

[1] H. Dimigen, H. Hubsch, R. Memming, Appl. Phys. Lett. 50 (1987) 1056.
[2] D.P. Monagan, D.G. Teer, P.A. Logan, I. Efeoglu, R.D. Amell, Surf. Coat. Technol. 60 (1993) 525.
[3] K.I. Schiffmann, M. Fryda, G. Goerigk, R. Lauer, P. Hinze, A. Bulack, Thin Solid Films 347 (1999) 60.
[4] A.A. Voevodin, J.P. O'Neill, S.V. Prasad, J.S. Zabinski, J. Vac. Sci. Technol., A, Vac. Surf. Films 17 (1999) 986.
[5] Q. Wei, R.J. Narayan, A.K. Sharma, J. Sankar, J. Narayan, J. Vac. Sci. Technol., A, Vac. Surf. Films 17 (1999) 3406.
[6] A.A. Voevodin, S.V. Prasad, J.S. Zabinski, J. Appl. Phys. 82 (1997) 855.
[7] D. Klaffke, A. Skopp, Surf. Coat. Technol. 98 (1998) 953.
[8] A.A. Voevodin, S.V. Prasad, J.S. Zabinski, J. Appl. Phys. 82 (1997) 855.
[9] K. Bewilogua, C.V. Cooper, C. Specht, J. Schroder, R. Wittorf, M. Grischke, Surf. Coat. Technol. 127 (2000) 224.
[10] H. Dimigen, C.P. Klages, Surf. Coat. Technol. 49 (1991) 543.
[11] S. Veprek, M. Haussmann, S. Reiprich, J. Vac. Sci. Technol., A, Vac. Surf. Films 14 (1996) 46.
[12] J. Frenkel, Phys. Rev. 54 (1938) 647.
[13] Q.F. Huang, S.F. Yoon, E. Rusli, H. Yang, B. Gan, K. Chew, J. Ahn, J. Appl. Phys. 88 (2000) 4191.

[14] A.A. Voevodin, M.A. Capano, S.J.P. Laube, M.S. Donley, J.S. Zabinski, Thin Solid Films 298 (1997) 107.
[15] C. Benndorf, M. Grischke, H. Koeberle, R. Memming, A. Brauer, F. Thieme, Surf. Coat. Technol. 36 (1998) 171.
[16] P.K. Srivastava, T.V. Rao, V.D. Vankar, K.L. Chopra, J. Vac. Sci. Technol., A, Vac. Surf. Films 2 (1984) 1261.
[17] E. Rusil, S.F. Yoon, Q.F. Huang, H. Yang, M.B. Yu, J. Ahn, Q. Zhang, E.J. Teo, T. Osipowicz, F. Watt, J. Appl. Phys. 88 (2000) 3699.
[18] S.F. Yoon, Q.F. Huang, E. Rusli, H. Yang, J. Ahn, Q. Zhang, C. Blomfield, B. Tielsch, L.Y.C. Tan, J. Appl. Phys. 86 (1999) 4871.
[19] X.B. Tian, T. Zhang, Z.M. Zeng, B.Y. Tang, P.K. Chu, J. Vac. Sci. Technol., A, Vac. Surf. Films 17 (1999) 3255.
[20] X.B. Tian, L.P. Wang, Q.Y. Zhang, P.K. Chu, Thin Solid Films 390 (2001) 139.
[21] X.B. Tian, R.K.Y. Fu, P.K. Chu, J. Vac. Sci. Technol., A, Vac. Surf. Films 20 (2002) 160.
[22] T. Zhang, P.K. Chu, R.K.Y. Fu, I.G. Brown, J. Phys., D Appl. Phys. 35 (2002) 3176.
[23] D.T.K. Kwok, T. Zhang, P.K. Chu, M.M.M. Bilek, A. Vizir, I.G. Brown, Appl. Phys. Lett. 78 (2001) 422.
[24] L. Doolittle, Nucl. Instrum. Methods Phys. Res., B Beam Interact. Mater. Atoms 9 (1985) 344.
[25] W.J. Meng, T.J. Curtis, L.E. Rehn, P.M. Baldo, J. Appl. Phys. 83 (1998) 6076.
[26] X.B. Tian, L.P. Wang, R.K.Y. Fu, P.K. Chu, Mater. Sci. Eng., A Struct. Mater.: Prop. Microstruct. Process. 337 (2002) 236.
[27] M.C. Bursell, Y.S. Lin, K.S. Cole, J. Vac. Sci. Technol., A, Vac. Surf. Films 4 (1986) 2459.
[28] J. Patt, D.J. Moon, C. Phillips, L. Thompson, Catal. Letters 65 (2000) 193.
[29] W.J. Yang, Y.H. Choa, T. Sekino, K.B. Shim, K. Niihara, K.H. Auh, Thin Solid Films 434 (2003) 49.
[30] P. Yang, S.C.H. Kwok, R.K.Y. Fu, Y.X. Leng, J. Wang, G.J. Wan, N. Huang, Y. Leng, P.K. Chu, Surf. Coat. Technol. 177 (2004) 747.